

Signal Propagation Modeling Based on Weighting Coefficients Method in Underground Tunnels

Yusuf Karaca¹ and Özgür Tamer²

¹Graduate School of Natural and Applied Sciences
Dokuz Eylül University, İzmir, Turkey
yusuf.karaca@deu.edu.tr

²Department of Electrical and Electronics Engineering
Dokuz Eylül University, İzmir, Turkey
ozgur.tamer@deu.edu.tr

Abstract — The propagation of electromagnetic waves guided in tunnels and mines is an area of scientific study which is hard to model due to multiple reflections on walls and surrounding obstacles. A novel propagation model for underground tunnels based on the weighting sum of the log-distance propagation model, the modified waveguide model and, the far zone propagation model for the ultra-high frequency (UHF) band is proposed in this paper. The propagation model is divided into five regions based on the distance between the transmitter and the receiver. Each region shows a different propagation characteristic and modeled with weighting sum of the base propagation models. Our model was tested in a tunnel with 2 m x 1.5 m cross-section and 250 m length. Measurement results are consistent with the proposed propagation model.

Index Terms — Propagation modeling, underground tunnel, underground communications.

I. INTRODUCTION

Modelling of electromagnetic wave propagation in underground environments has been an active area of research for many years. Despite several theoretical analyses and experimental studies, electromagnetic wave propagation in underground tunnels is hard to model with high precision and low complexity due to the imperfect structure of the surrounding obstacles and walls, such as multiple reflections from the surrounding walls [1]. A large number of models were presented and discussed for underground tunnels [2]. Zhang and Hong proposed a model based on the ray optical propagation model to show signal propagation at the UHF frequency band for rectangular underground tunnels [3]. Zhang, Zheng, and Sheng modeled electromagnetic wave propagation at 900 MHz using free space and mod propagation models for coal mines [4]. Two propagation regions with different characteristics were defined,

where the breakpoint between the regions in the passageways was found to be 45 m from the transmitter. The waveguide propagation model for coal mines is proposed by Emslie, Lagace, and Strong [5]. The waveguide model is investigated in rectangular coal tunnels at frequencies 1 GHz and 415 MHz for both vertical polarization and horizontal polarization. Boutin et al. also present breakpoints for different propagation models [6]. Guan and friends showed that the free-space propagation model can be used at short ranges, while the multimode propagation model can be used at medium range distances and the fundamental mode propagation model can be used for longer ranges [7]. This model proposes a solution to unify and extend existing propagation mechanism models in tunnels. Although many researchers prefer a waveguide-based model to interpret the electromagnetic wave propagation in the far region [5], the results are not satisfactory for long tunnels. If the transmitter and receiver are far enough from each other, propagation is more similar to the far zone propagation model [7]. In fact, far zone propagation was not sufficiently investigated by researchers due to a lack of experimental studies in long tunnels in underground environments. Rak and Pechac searched for experimental measurements of subterranean galleries for two frequencies: 446 MHz and 860 MHz [8]. They proposed a simple linear attenuation model using recorded experimental data.

In this paper, a novel propagation model based on a combination of three different propagation mechanisms for near, mid, and far regions is introduced. A gradual transition with the weighting coefficients is applied between propagation regions. In the second part of the paper, a theoretical background about the employed propagation models is presented and the proposed propagation model is introduced in section three. A comparison of the model with measurement results is presented in the fourth section while the results are

concluded in the fifth and the final section.

II. THEORETICAL BACKGROUND

The signal propagation model proposed in this work employs three different propagation models introduced in below subsections.

A. Log-distance path loss model

In the near zone of tunnel-like structures, the slope of the signal attenuation curve is steep [6]. In our study we adopt the log-distance signal propagation model in the near zone given in equation (1) [9]:

$$P_1 = \overline{PL}(d_0) + 10n \log_{10} \left(\frac{d}{d_0} \right), \quad (1)$$

where n is the path loss exponent, d is the transmitter-receiver separation in meters, d_0 is the distance of the reference measurement and $\overline{PL}(d_0)$ is the path loss at d_0 . Path loss exponent value is used as 1.75 since there is line-of-sight between the transmitter and the receiver and the tunnel is a rectangular cross-section one [9], while the value of the d_0 is 1 m. Received power for the log distance model (P^{Log}) is given by:

$$P^{Log} = \sum_{i=1}^{+\infty} A_i P_1, \quad (2)$$

where A_i are the weighting coefficients and P^{Log} is the representation of weighting signal attenuation for the near zone.

In the proposed model, log-distance is the dominant propagation mode for the first 50λ of the distance from the transmitter where λ is the wavelength as presented in Fig. 6. The attenuation of the signal based on this propagation model is presented in Fig. 2, Fig. 3 and Fig. 4.

B. Waveguide model

We consider that the tunnel is similar to a waveguide for the preferred frequency band as presented in the literature [5], [10]. Walls are lossy media built of concrete and iron bars with the corresponding electrical parameters defined in Fig. 1 as ε_ℓ , μ_ℓ , σ_ℓ , and ε_b , μ_b , σ_b . E^i , H^i , E^r , H^r in Fig. 1 are defined as the fields in the space of the waveguide-like structure. while E_b^{tr} , H_b^{tr} are the fields on top and bottom of the tunnel walls E_ℓ^{tr} , H_ℓ^{tr} are fields at the left and right of tunnel walls. Electrical space inside the rectangular waveguide is $\varepsilon_r=1$, $\mu_r=1$ since the tunnel is filled with air. The horizontal and vertical dimensions of the waveguide are given as a and b respectively, while the horizontal lines on axis x for the model and the vertical lines on axis y and the wave

propagates in the z -direction.

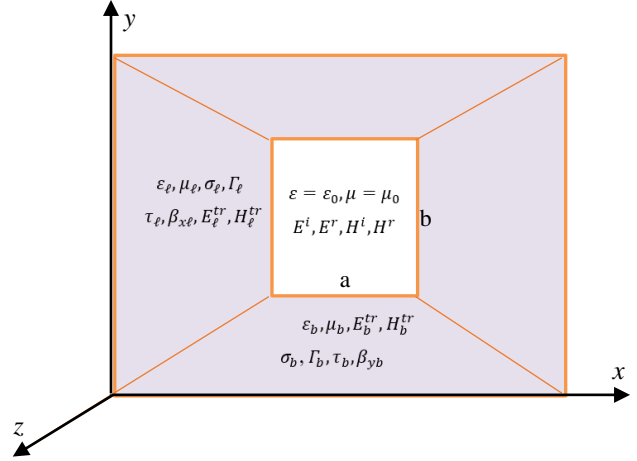


Fig. 1. Cross-section of the tunnel as a waveguide.

The complex dielectric constant for the sidewalls is given by the following equation:

$$\varepsilon_\ell = \varepsilon_\ell' - j \frac{\sigma_\ell}{\omega}, \quad (3)$$

where σ_ℓ is the conductivity of the sidewalls. Experimental studies show that ε_ℓ' is a real dielectric constant [14] while ω is working frequency [11]. Similarly, the dielectric constant for the top and bottom walls is defined as:

$$\varepsilon_b = \varepsilon_b' - j \frac{\sigma_b}{\omega}, \quad (4)$$

where σ_b is the conductivity of the top and the bottom where ε_b' is the real dielectric constant parameter.

The reflection coefficient on the sidewalls (Γ_ℓ) and the top and bottom walls (Γ_b) is given by:

$$\Gamma_\ell = \frac{\sqrt{\varepsilon} - \sqrt{\varepsilon_\ell}}{\sqrt{\varepsilon} + \sqrt{\varepsilon_\ell}}, \quad (5)$$

$$\Gamma_b = \frac{\sqrt{\varepsilon} - \sqrt{\varepsilon_b}}{\sqrt{\varepsilon} + \sqrt{\varepsilon_b}}. \quad (6)$$

The transmission coefficients for the sidewalls (τ_ℓ) and the top and bottom walls (τ_b) are given as:

$$\tau_\ell = \left(\frac{1}{\varepsilon} + \frac{\Gamma_\ell}{\varepsilon} \right) \frac{\beta_x \varepsilon_\ell}{\beta_x \varepsilon_\ell}, \quad (7)$$

$$\tau_b = \left(\frac{1}{\varepsilon} + \frac{\Gamma_b}{\varepsilon} \right) \frac{\varepsilon_b \beta_y}{\beta_y b}, \quad (8)$$

where β_{xb} is the phase constant for the sidewalls, β_{yb} is the phase constant for the top and bottom walls and β_y is the phase constant for the tunnel cavity.

The direction of the power flow is defined in the $+z$ direction as presented in Fig. 1. Power flow, P_{mn} , of an electromagnetic wave in TE_{mn}^z mode along the axis of $+z$ is presented in equation (9) [13].

Table 1: Regions of the weighting signal propagation model

Log-distance Path Loss Model (P^{Log})	Transient Region I ($P^{Log} + P^{Waveg}$)	Waveguide Model (P^{Waveg})	Transient Region II ($P^{Waveg} + P^{Far}$)	Far Zone Propagation Model (P^{Far})
$<50\lambda$	$50\lambda-120\lambda$	$120\lambda-700\lambda$	$700\lambda-800\lambda$	$>800\lambda$

$$P_{mn} = \frac{A_{mn}^2 \beta_z}{2\omega\mu\epsilon^2} \left[\beta_x^2 \left(\frac{b \sin(2n\pi)}{4n\pi} + \frac{b}{2} \right) \left(\frac{a}{2} - \frac{a \sin(2m\pi)}{4m\pi} \right) + \beta_y^2 \left(\frac{a \sin(2m\pi)}{4m\pi} + \frac{a}{2} \right) \left(\frac{b}{2} - \frac{b \sin(2n\pi)}{4n\pi} \right) \right], \quad (9)$$

where β_z is the phase constant in the +z direction.

The real part of surface impedance for the sidewalls is given in equation (10) and the power losses because of the conductivity is given in equation (11). It is assumed that the dissipated power for both the left wall and the right walls are the same:

$$R_{s\ell} = \sqrt{\frac{\omega\mu_\ell}{2\sigma_\ell}}, \quad (10)$$

$$\frac{P_{c\ell}}{z_0} = \frac{R_{s\ell} A_{mn}^2}{2(2\omega\mu_0)^2} \left| \frac{1}{\epsilon} + \frac{\Gamma_\ell}{\epsilon} - \frac{\tau_\ell}{\epsilon_\ell} \right|^2 \left\{ \left(\frac{b \sin(2n\pi)}{4n\pi} + \frac{b}{2} \right) \beta_c^4 + \left(\frac{b}{2} - \frac{b \sin(2n\pi)}{4n\pi} \right) \beta_y^2 \beta_z^2 \right\}. \quad (11)$$

Here $P_{c\ell}$ is the dissipated power on the sidewalls due to conductivity, β_c is the cutoff phase constant, μ_0 is the permeability of the air medium in the tunnel. The conduction losses on the top and bottom surface, P_{cb} , is given by:

$$\frac{P_{cb}}{z_0} = \frac{R_{sb} A_{mn}^2}{2(2\omega\mu_0)^2} \left| \frac{1}{\epsilon} + \frac{\Gamma_b}{\epsilon} - \frac{\tau_b}{\epsilon_b} \right|^2 \left\{ (\beta_x \beta_z)^2 \left(\frac{a}{2} - \frac{a \sin(2m\pi)}{4m\pi} \right) + \beta_c^4 \left(\frac{a \sin(2m\pi)}{4m\pi} + \frac{a}{2} \right) \right\}, \quad (12)$$

where P_c is the total loss in equation (13) and perturbational method is preferred as presented in equation (13):

$$\alpha_c = \frac{P_c/z_0}{2P_{mn}} = \frac{\left(\frac{2P_{cb}}{z_0} + \frac{2P_{c\ell}}{z_0} \right)}{2P_{mn}} = \frac{P_{c\ell} + P_{cb}}{z_0 P_{mn}}. \quad (13)$$

In order to find the total conduction losses associated with a rectangular waveguide, surface currents are obtained by using cross product of the magnetic field and normal unity vector along the x-z plane at the $y=0$, $y=b$ and y-z plane at the $x=0$, $x=a$ respectively. Total linear surface currents are obtained by means of magnetic fields on the surfaces and the total conduction losses are evaluated by integrating scalar product of the linear surface currents along the all four surfaces and the losses on the four walls are evaluated as total conduction losses (P_c) accordingly. Since the top and bottom losses are assumed as equal, total losses on these walls is equal to $2 \cdot P_{cb}$ and sidewalls losses are also assumed equal and total losses on the sidewalls is equal to $2 \cdot P_{c\ell}$. The received power is therefore given by:

$$P_2 = P_0 \exp(-2\alpha_c z), \quad (14)$$

where P_0 is the reference power. The weighting signal attenuation for the waveguide model is given by:

$$P^{Waveg} = \sum_{i=1}^{+\infty} B_i P_2, \quad (15)$$

where B_i are the weighting coefficients.

C. Far region propagation

Far region signal propagation model is given by the following equation:

$$P_3 \cong \frac{A_0^2 ab}{2\eta_0 d^2}, \quad (16)$$

where A_0 is the constant of the integration from a differential equation. a and b are the tunnel cross-section dimensions, d is the distance from the transmitter to the receiver antennas, and η_0 is the intrinsic impedance of the free space (the propagation medium) [12]. Received power for the far zone (P^{Far}) is given by:

$$P^{Far} = \sum_{i=1}^{+\infty} C_i P_3, \quad (17)$$

where C_i are the corresponding weighting coefficients.

Far region propagation model comparison with other models and signal measurements is presented in Fig. 2, Fig. 3 and Fig. 4.

III. COMBINED PROPAGATION MODEL

As can be observed from Fig. 2, 3 and 4 each propagation model presents a different propagation characteristic, and it is not possible to use just a single one to model the propagation in a tunnel since signal level at different distances match different propagation models through the tunnel. This case is also verified by the usage of the measurements presented in Fig. 7. Therefore, a new model which is a combination of the three models is proposed in this study. The tunnel is divided into five zones, three of them have dominant propagation models, and two are transient regions between the dominant models as presented in Table 1. The propagation models presented in Section II are used with different weighting coefficients in these zones. The propagation model for the first and the closest distance region is the log-distance path loss model. For the second part propagation model gradually transforms from the log-distance path loss model to the waveguide-based propagation model. The propagation model for the third region is defined by the waveguide model is also proposed in this paper which is calculated via the perturbation method [13]. The fourth region is a transient region transforming gradually to the far zone propagation model from the proposed waveguide model. The

weighting coefficients of both the waveguide model and the far zone signal model are the same in the fourth region. For the fifth and the farthest region, the far zone propagation model is preferred.

IV. MEASUREMENT RESULTS

Signal measurements were taken at the heating infrastructure tunnels of the Karamanoğlu Mehmetbey University, which was built as a rectangular-shaped tunnel. The underground tunnel has a cross-section of 2 m x 1.5 m. The overall width of the tunnel is 1.5 m including the pipes. Pipes are not taken into account on signal propagation since they are thick plastic pipes carrying water. The total length of the tunnel is 250 m including concrete walls supported with iron bars. Measurements were taken with an Anritsu MG3694C as the transmitter and an Anritsu MS2830A as the receiver. A photograph taken during measurements is presented in Fig. 5. Measurements are carried out at 980 MHz, 1000 MHz and 1150 MHz and both of the antennas are placed at a height of 1.5 m to imitate an average person's communication equipment height. Measurement results and their comparison with the propagation models are presented in Fig. 2, Fig. 3 and Fig. 4. It can be observed that none of the pre-mentioned propagation models had compatibility with the measurement results, but they do comply with the measurements at specific distances. For the closest part, the log-distance propagation model shows a good match while for most of the graph, the waveguide model shows a good match between 120λ and 700λ for the measurement. After 700λ the model is closer to the far region propagation model. The distances comply with the proposed model, then we need to determine the weights for the transient region I and II in Table 1.

As presented in Table 1, the first region is between 0λ and 50λ . For the first region, the propagation model is dominant as mentioned before while for region three in Table 1 waveguide propagation model is dominant from 120λ until 700λ . Therefore, the second region starts at 50λ and ends at 120λ . For the second region, a transition between these two models is necessary, as presented in Table 1 weighting coefficients (in Fig. 6) provide a gradual transition between the two models. After the third region, we again need a gradual transition between the waveguide model and the far region model.

This transition is different from the first transition in most of the second transition region in Table 1 waveguide model and the far region model are equally weighted. In our measurements, it was not possible to take any measurements in region 5 in Table 1 due to the physical limitations of the tunnel, but measurement results presented in Fig. 2, Fig. 3 and Fig. 4 show a better match with the far region propagation model at the end of the tunnel. A comparison between the measurement results and the proposed model is presented in Fig. 7. As can be observed the model fits the measurement results. The

error of the measurements is calculated and compared for different frequencies along the z-axis in Fig. 8.

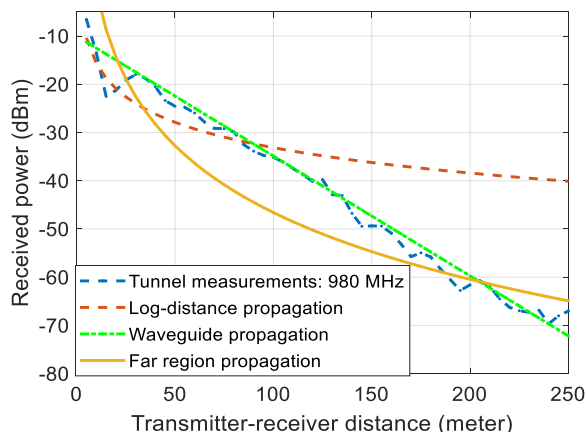


Fig. 2 Path loss of the propagation models and measurements for 980 MHz.

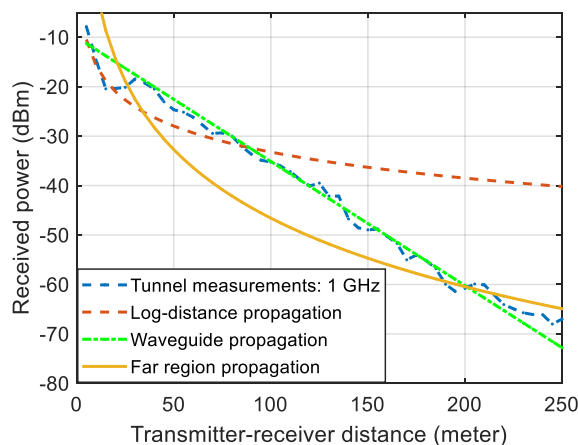


Fig. 3 Path loss of the propagation models and measurements for 1000 MHz.

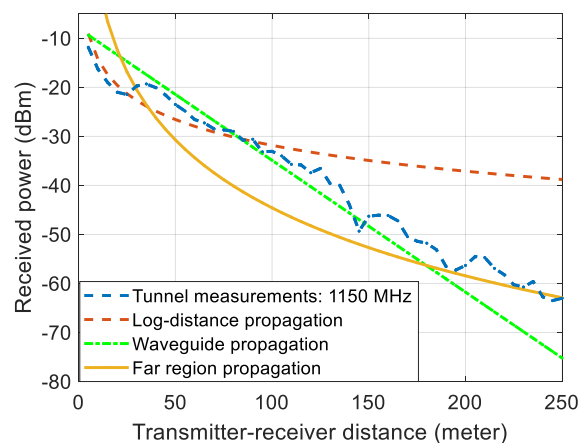


Fig. 4. Path loss of the propagation models and measurements for 1150 MHz.



Fig. 5. Signal measurements and underground tunnel.

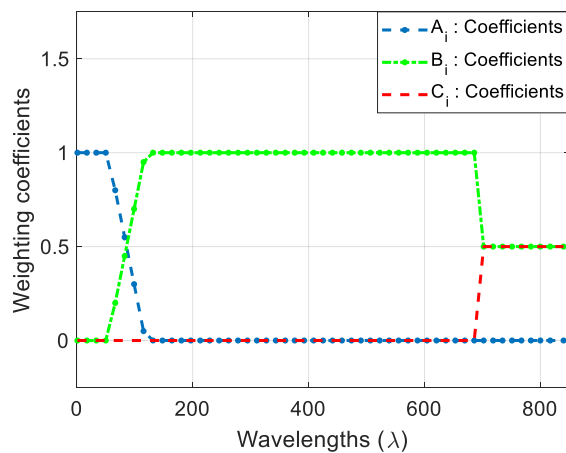


Fig. 6. Applied weighting coefficients for the regions.

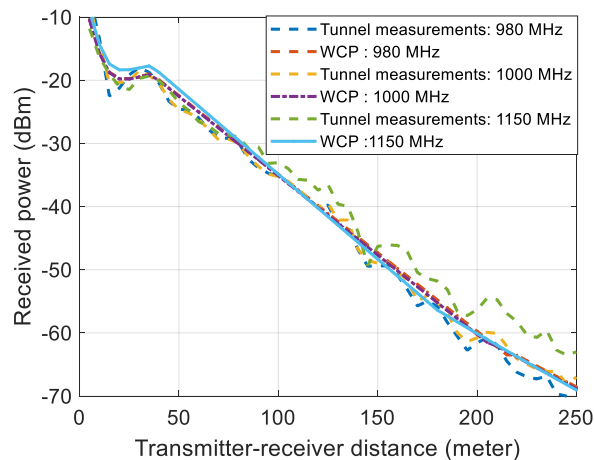


Fig. 7. Comparison of the signal measurements and weighting coefficient propagation models.

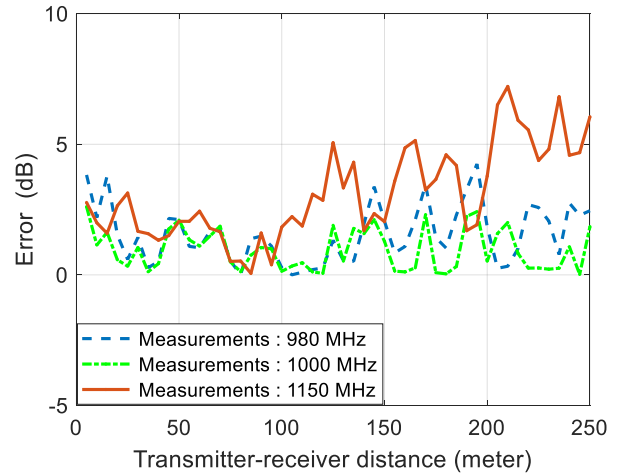


Fig. 8. Error comparison for different frequencies.

V. CONCLUSION

A novel radio wave propagation model is introduced for rectangular cross-section tunnels in this paper. The model is based on the idea of separating the propagation medium into five regions with different propagation characteristics based on the distance in terms of wavelength between the transmitter and the receiver. Three areas of the propagation model have dominant propagation characteristics when two regions are transition regions among the three regions. The transient region propagation models are weighted, which improves the consistency of the proposed model. A waveguide signal model used in the second, third, and fourth regions a novel propagation model proposed for tunnel propagation at UHF frequency band. Measurements are conducted at 980 MHz, 1000 MHz and 1150 MHz in a tunnel of the heating system. According to the results, the proposed signal propagation model complies with the underground signal measurement values. It was possible to validate the model in the fifth region at 1150 MHz since the wavelength is smaller and the length of the tunnel is barely enough for this frequency.

REFERENCES

- [1] A. E. Forooshani, S. Bashir, D. G. Michelson, and S. Noghianian, "A survey of wireless communications and propagation modeling in underground mines," *IEEE Commun. Surv. Tutorials*, vol. 15, no. 4, pp. 1524-1545, 2013.
- [2] A. Hrovat, G. Kandus, and T. Javornik, "A Survey of radio propagation modeling for tunnels," *IEEE Commun. Surv. Tutorials*, vol. 16, no. 2, pp. 658-669, 2014.
- [3] Y. P. Zhang and H. J. Hong, "Ray-optical modeling

- of simulcast radio propagation channels in tunnels,” *IEEE Trans. Veh. Technol.*, vol. 53, no. 6, pp. 1800-1808, 2004.
- [4] Y. P. Zhang, G. X. Zheng, and J. H. Sheng, “Radio propagation at 900 MHz in underground coal mines,” *IEEE Trans. Antennas Propag.*, vol. 49, no. 5, pp. 757-762, 2001.
- [5] A. G. Emslie, R. L. Lagace, and P. F. Strong, “Theory of the propagation of UHF radio waves in coal mine tunnels,” *IEEE Trans. Antennas Propag.*, vol. 23, no. 2, pp. 192-205, 1975.
- [6] M. Boutin, A. Benzakour, C. L. Despins, and S. Affes, “Radio wave characterization and modeling in underground mine tunnels,” *IEEE Trans. Antennas Propag.*, vol. 56, no. 2, pp. 540-549, 2008.
- [7] K. Guan and Z. Zhong, “Complete propagation model structure in-side tunnels,” *Prog. Electromagn. Res.*, vol. 141, pp. 711-726, 2013.
- [8] M. Rak and P. Pechac, “UHF propagation in caves and subterranean galleries,” *IEEE Trans. Antennas Propag.*, vol. 55, no. 4, pp. 1134-1138, 2007.
- [9] H. I. Volos, C. R. Anderson, W. C. Headley, R. M. Buehrer, C. R. C. M. Da Silva, and A. Nieto, “Preliminary UWB propagation measurements in an underground limestone mine,” *GLOBECOM - IEEE Glob. Telecommun. Conf.*, pp. 3770-3774, 2007.
- [10] O. M. Abo Seida, “Propagation of electromagnetic waves in a rectangular tunnel,” *Appl. Math. Comput.*, vol. 136, no. 2-3, pp. 405-413, 2003.
- [11] N. R. Peplinski, F. T. Ulaby, and M. C. Dobson, “Dielectric properties of soils in the 0.3–1.3-GHz range,” *IEEE Trans. Geosci. Remote Sens.*, vol. 33, no. 3, pp. 803-807, 1995.
- [12] J. Molina-Garcia-Pardo, J. Rodriguez, and L. Juan-Llacer, “Wide-band measurements and characterization at 2.1 GHz while entering in a small tunnel,” in *IEEE Transactions on Vehicular Technology*, vol. 53, no. 6, pp. 1794-1799, 2004.
- [13] D. Pozar, *Microwave Engineering*. 3rd ed., John Wiley and Sons, 2005.
- [14] M. Ozturk, U. K. Sevim, O. Akgol, E. Unal, and M. Karaaslan, “Determination of physical properties of concrete by using microwave nondestructive techniques,” *Applied Computational Electromagnetics Society Journal*, vol. 33, no. 3, pp. 265-272, 2018.



Yusuf Karaca received his B.S. degree from the Department of Electronic Engineering, Uludağ University, in 2010, Bursa, Istanbul, Turkey and M.S. degree from Department of Electrical-Electronics Engineering, Istanbul University, in 2014, Istanbul, Turkey. Currently, he is a graduate Research Assistant School of Department of Electrical-Electronics Engineering, Dokuz Eylül University, İzmir, Turkey. He is pursuing a Ph.D. degree under the supervision of Asst. Prof. Özgür Tamer. His current research interests are in Electromagnetic Wave Propagation, Wireless Underground Communication Networks, and Wireless Sensor Networks.



Özgür TAMER received his BSc., MSc. in and Ph.D. at Dokuz Eylül University Electrical and Electronics Eng. Dept in 1997, 2001, and 2008 respectively. He worked at NTNU Telematics Department at Trondheim/Norway as a postdoc researcher from 2010-2011 He is currently working as an Assistant Professor at Dokuz Eylül University Electrical and Electronics Eng. Dept. İzmir/Turkey. His main research interests are focused on smart antenna systems, embedded systems, and wireless sensor networks.